Science Bulletin 64 (2019) 1426–1435

Contents lists available at ScienceDirect

Science Bulletin

journal homepage: www.elsevier.com/locate/scib

Review

Approaching ohmic contact to two-dimensional semiconductors

Kailang Liu, Peng Luo, Wei Han, Sanjun Yang, Shasha Zhou, Huiqiao Li, Tianyou Zhai *

State Key Laboratory of Material Processing and Die & Mould Technology, School of Material Sciences and Engineering, Huazhong University of Science and Technology, Wuhan 430074, China

ARTICLE INFO

Article history:
Received 2 April 2019
Received in revised form 26 May 2019
Accepted 19 June 2019
Available online 26 June 2019

Keywords:
Two-dimensional semiconductor
Ohmic contact
Fermi level pinning
Schottky barrier

ABSTRACT

Two-dimensional semiconductors have attracted immense research interests owing to their intriguing properties and promising applications in electronic and optoelectronic devices. However, the performance of these devices is drastically hindered by the large Schottky barrier at the electric contact interface, which is hardly tunable due to the Fermi level pinning effect. In this review, we will analyze the root causes of the contact problems for the two-dimensional semiconductor devices and summarize the strategies on the basis of different contact geometries, aiming to lift out the Fermi level pinning effect and achieve the ohmic contact. Moreover, the remarkable improvement of the device performance thanks to these optimized contacts will be emphasized. At the end, the merits and limitations of these strategies will be discussed as well, which potentially gives a guideline for handling the electric contact issues in two-dimensional semiconductors devices.

1. Introduction

Inspired by the isolation of graphene in 2004, various two-dimensional (2D) materials have been rediscovered by researchers since they possess novel properties with respect to their bulk non-layered counterparts [1]. Among them, the two-dimensional semiconductors (2DS) such as the transition metal dichalcogenides (MoS_2 [2,3], WSe_2 [4,5], $ReSe_2$ [6]), anisotropic black phosphorus [7–9] and GeP [10,11] have been intensively studied and some novel properties including the tunable band gap [12], the indirect-to-direct band gap transition [2], the formation of strongly-bounded excitons [13], the light-valley interactions [14] and highly gate controllability [15] due to the atomic thinness have been demonstrated and investigated. These novel properties not only imply promising applications in electronic and optoelectronic devices [16–21], but also provide platforms to design novel devices for the study of fundamental physics [22–24]. Nevertheless, the performances of these novel devices based on 2DS and the 2DS heterostructure [18,25] are usually limited by large Schottky barrier (SB) at the electric contact which connects the 2D materials with external circuitry [26,27], and the intrinsic properties of 2DS can be totally obscured because of the large contact resistance [28]. Reducing the Schottky barrier and achieving the ohmic contact turn to be the prerequisite for optimizing the device performances and studying the intrinsic physical properties of 2DS.

Unlike the non-layered bulk semiconductors, 2DS tend to form an interface of totally different configurations because of the absence of dangling bonds on the surface when coming in contact with metal electrodes [26]. The interface configurations actually determine the band structure at the interface and the contact resistance, thus govern the charge flow and device performance as a whole. Depending on the interface configuration, the contact can be classified into three different geometries (Fig. 1). First, we introduce the top contact, the most-used contact geometry, and by the way revisit the root causes of large SB and Fermi level pinning effect (FLPE) in this conventional contact geometry. Some reported strategies to reduce the SB based on this analysis will be reviewed. Then, the van der Waals (vdW) contact will be reviewed. This new contact geometry has been developed thanks to the discovery of new layered metallic materials and the assemble techniques of vdW heterostructure. The metallic electrodes of vdW contact are usually atomic thin and their Fermi levels are thus gate-controllable, which opens up opportunities of great interest for novel device design. The third contact geometry we will emphasize is the edge contact, in which the metal electrodes only contact to the exposed edges with dangling bonds so that covalent bonds form between the atoms of electrodes and 2DS edges, leading to the reduction of the contact resistance. Different approaches used to realize the edge contact geometry will be reviewed respectively. In this review, we focus particularly on the strategies of the ohmic contact fabrication, while the physical mechanisms of charge carriers flow through the contact regarding the different contact configurations will be neglected, which have been summarized by Allain et al. [26] and systematically studied by Kang et al. [29].

* Corresponding author.
E-mail address: zhaity@hust.edu.cn (T. Zhai).

https://doi.org/10.1016/j.scib.2019.06.021
2095-9273/

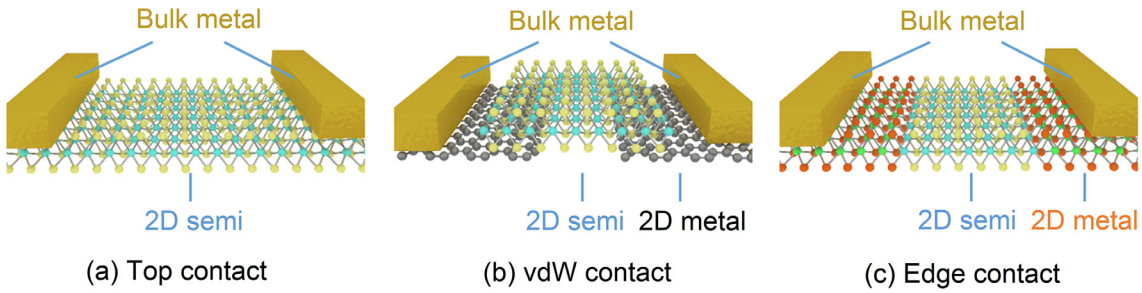

Fig. 1. (Color online) Three contact geometries to 2DS. The schematic figures of (a) the conventional top contact: bulk metal contacts (usually by deposition) with the surface of 2DS; (b) the vdW contact: 2D metallic (or semi-metallic) materials contact with the 2DS via a plane-to-plane vdW interaction; and (c) the edge contact: metallic materials contact with the 2DS from their edges with the formation of bonds at the interface.

2. Approaching ohmic contact

The contact issues between 2DS and metallic electrodes arise from the metal–semiconductor junctions (MSJ) [30]. The MSJ is ubiquitous in the electronic and optoelectronic devices since they connect the flow of charges within semiconductor and the external circuitry [26,30]. The high-quality contact allows the low-resistance flow of charges, which is determined by the SB at the contact interface [26,30–32]. The Schottky barrier height (Φ) is the energy barrier that charges need to overcome while drifting between metal electrodes and semiconductor, which, in the ideal case, is predicted by the Schottky-Mott rule [33,34]:

$$\Phi_e = W - X_s, \quad (1)$$

$$\Phi_h = I_s - W, \quad (2)$$

where Φ_e and Φ_h are the Schottky barrier height for electrons and holes respectively, W is the work function of electrode metal, and X_s, I_s stand for the electron affinity and ionization potential of semiconductor. According to Schottky-Mott rule, for an arbitrary semiconductor, one can reduce SB height Φ_e and Φ_h through simply choosing the electrode metal of suitable work function W. This prediction, however, can hardly be fulfilled experimentally as Φ_e and Φ_h vary little with respect to W and the Fermi level is usually pinned at a fixed position between the semiconductor band gap (Fig. 2a), leaving a large Φ_e and Φ_h uncontrollable with metals of various W. This so-called FLPE can be characterized by a pinning factor S.

$$S = |d\Phi/dW|, \quad (3)$$

where S should be equal to 1 according to Schottky-Mott rule. The experiments, nevertheless, reveal that the S is merely 0.07 and 0.11 for monolayer $MoTe_2$ and monolayer MoS_2 respectively (Fig. 2b), indicating the existence of a strong FLPE [35]. The FLPE is actually intensively studied in conventional semiconductor devices, which stems from many factors, such as the metal-induced gap states (MIGS), the impurities and chemical disorder at the interface, interface dipoles due to the charge transfer between the MSJ [27,31,36]. It has been found to be a difficult task to eliminate these problems via the conventional fabrication processes since the residues, defects, strain or the discontinuity of crystal surface will be left at the MSJ interface after the processes such as lithography and metal deposition. Liu et al. [27] however demonstrated a method to avoid these problems by transferring the electrodes onto the 2DS. They found that the MSJ interface was free of defects or chemical residues and the crystal lattice remain pristine thanks to the non-contaminant fabrication process and the weak vdW interaction at the MSJ interface, see the comparison between the transferred contact (Fig. 2c) and the deposited contact (Fig. 2d). Using different metals, the Φ_e and Φ_h can be extracted from the device measurement, which is then plotted with respect to W (Fig. 2e). The fitting slope S_{tran} is found to be approximately 0.96, approaching the Schottky-Mott limit. In contrast, the S_{evap} for the deposited metal is 0.09, indicating a strong FLPE, which is attributed to MIGS, the defects and chemical disorders at the MSJ interface induced by the aggressive conventional fabrication process. It is thus obvious that the key to eliminate the FLPE is to engineer the MSJ interface and reduce the interaction between the metal atoms and 2DS.

2.1. Top contact using tunneling buffer layer

Based on the aforementioned analysis, it is crucial to retain the pristine surface of 2DS to unlock the FLPE in the top contact configuration [26,27]. In this regard, engineering the MSJ interface turns to be a possible solution. It has been reported that the FLPE can be alleviated by inserting an ultrathin buffer layer of oxide into at the interface of top contact metal and 2DS [37–39]. The buffer oxide acts as a tunneling layer at the contact interface. To achieve the effective spin injection into MoS_2 channel from Co contact, Chen et al. [37] used MgO of 2 nm as the contact tunneling layer and found the 84% reduction of SB height from 60.4 meV without the tunneling layer. Similar works of inserting ultrathin buffer layer of oxides (Ta_2O_5 [38], TiO_2 [39]) to reduce the FLPE have been reported. However, the experimental results revealed that the FLPE still remains despite of a significant alleviation. For instance, the TiO_2 buffer layer increase the pinning factor S from 0.02 to 0.24, but still far from the Schottky-Mott rule [39]. This may result from the dangling bonds of these non-layered buffer layers which possibly give rise to the interfacial gap states. It turns to be a better solution to use layered 2D materials as buffer layer, which could possibly furthermore reduce the gap states and achieve the ohmic contact. Farmanbar et al. [40,41] theoretically proposed a method that one single layer of layered materials is inserted between 2DS and top contact metal to break their direct interaction and destroy the strongly-bonded interface states (Fig. 3a–c). For instance, they found that when monolayer hexagonal boron nitride (h-BN) was placed between electrode metal cobalt (Co) and monolayer MoS_2 as a middle buffer layer, it not only eliminate the FLPE, but also shift the work function of Co by more than 1 eV, leading to the alignment of the Fermi level of CoBN contact and the bottom of MoS_2 conduction band [40]. They also verified the effect of the middle monolayer h-BN through calculating the band structures of the contact interface of CoBN/MoS_2 (Fig. 3c), and found that band structure of MoS_2 remained unperturbed due to the existence of the buffer layer h-BN.

Inspired by this theoretical work, Cui et al. [42] implemented the corresponding experiments to fabricate the low-resistance contact to monolayer MoS_2 (Fig. 3d). Monolayer MoS_2 was sandwiched between a monolayer h-BN and a multilayer h-BN via the reverted vdW assembly technique, and then Co and Au were

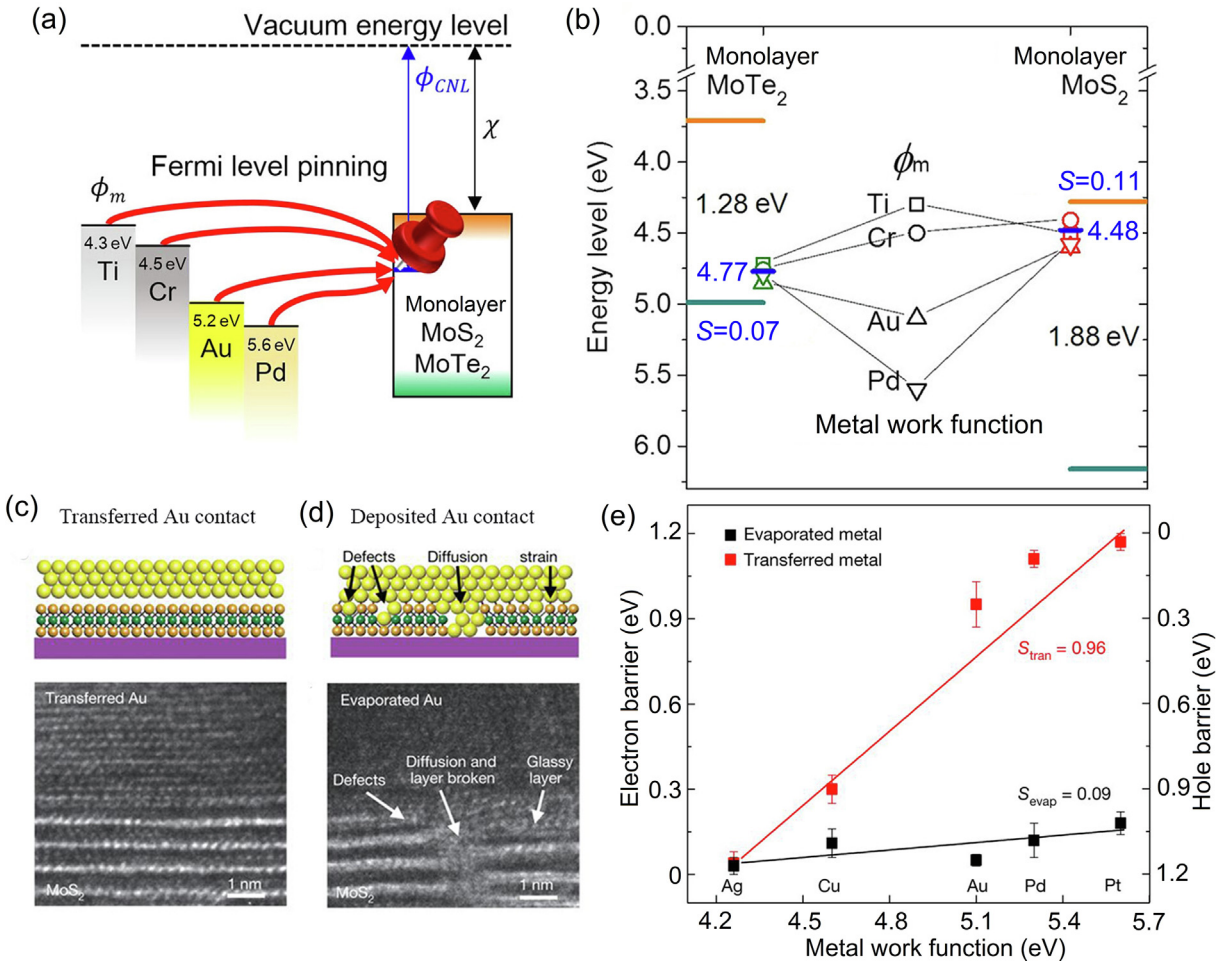

Fig. 2. (Color online) FLPE for the conventional top contact to 2DS. (a) The Fermi level is pinned at a fixed position within the band gap of monolayer MoS_2 and $MoTe_2$ for contact metals with different *W*. (b) The Fermi levels of various metals are pinned at a fixed position, around 4.77 and 4.48 eV , with pinning factor *S* equal to 0.07 and 0.11 respectively for monolayer $MoTe_2$ and MoS_2. Adapted from Ref. [35], Copyright © 2017 American Chemical Society. The schematic figures and cross-section high resolution transmission electron microscope (HRTEM) images of interface states for transferred (c) and deposited (d) metal contact, showing the defects and chemical disorders at the MSJ interface of deposited metal contact. (e) The FLPE parameter *S* is determined via the measurement of Φ with respect to *W*, with S_{tran} approaching the Mott-Schottky limit and S_{evap} showing strong FLPE. Adapted from Ref. [27], Copyright © 2018 Springer Nature Publishing.

deposited sequentially onto the monolayer h-BN to form the designed CoBN (Co on monolayer h-BN) contact. The gate-dependent transport measurement revealed that the resistance decreases with the decreasing temperature, showing a metallic conduction in channel and barrier-free contacts when the gate voltage is large enough (over 30 V). At low temperature and low carrier density, the CoBN contact shows the lowest contact resistance compared with the contacts via other methods (Fig. 3e). The Shubnikov-de Haas oscillations have also been successfully demonstrated thanks to this optimized contact. The contact of NiBN (Ni + h-BN) [43] and NiGr (Ni + graphene) [44] were also experimentally realized by Wang et al. and Leong et al. respectively and the remarkable reduction of SB height has been reported in these two works. The monolayer h-BN decreases the work function *W* of the metal, favorable for n-type ohmic contact. The possibilities to form p-type ohmic contact to 2DS are also exploited in another theoretical work [41]. For other layered materials besides h-BN attaching onto different metals, Farmanbar et al. [41] calculated their work function *W* (Fig. 3c). Interestingly, they found that NbS_2 attaching onto any metal forms a p-type ohmic contact to all the well-known TMD semiconductors. They attributed this phenomenon to the metallic nature of NbS_2 and its effect of increasing the work function of contact metal, contrary to the effect of insulator h-BN (Fig. 3c).

In principle, the choice of the ultra-thin buffer layer placed at the MSJ interface can be furthermore extended. Given that attaching the monolayer 2D materials onto 2DS requires the vdW assemble technique, which is still a time-consuming and low-yield process and unfavorable for large-scale fabrication, Cho et al. [45] reported the use of the thiol-molecules as the buffer layer instead of layered materials. The choice of this material allows inserting the buffer layer via selective vapor deposition instead of the complex transfer process, making the device fabrication much more convenient and opening up the possibility for scaling up.

2.2. vdW contact

Analogous to the top contact with 2D materials as middle buffer layer, the vdW contact can also significantly alleviate the FLPE due to its weak interaction at the interface with 2DS [42]. VdW contact is made of atomic thin metallic 2D materials assembled with 2DS (Fig. 1b). They contact with each other via vdW forces and the charge carriers flow via the tunneling mechanism through the vdW gaps. Because of the weak vdW interactions, the electronic states of 2DS remain pristine and the FLPE does not arise. Moreover, using the ultrathin 2D materials as contact gives more benefits in device design. First, the Fermi level of 2D contact materials can be readily tuned by gate or doping so that it can align with a

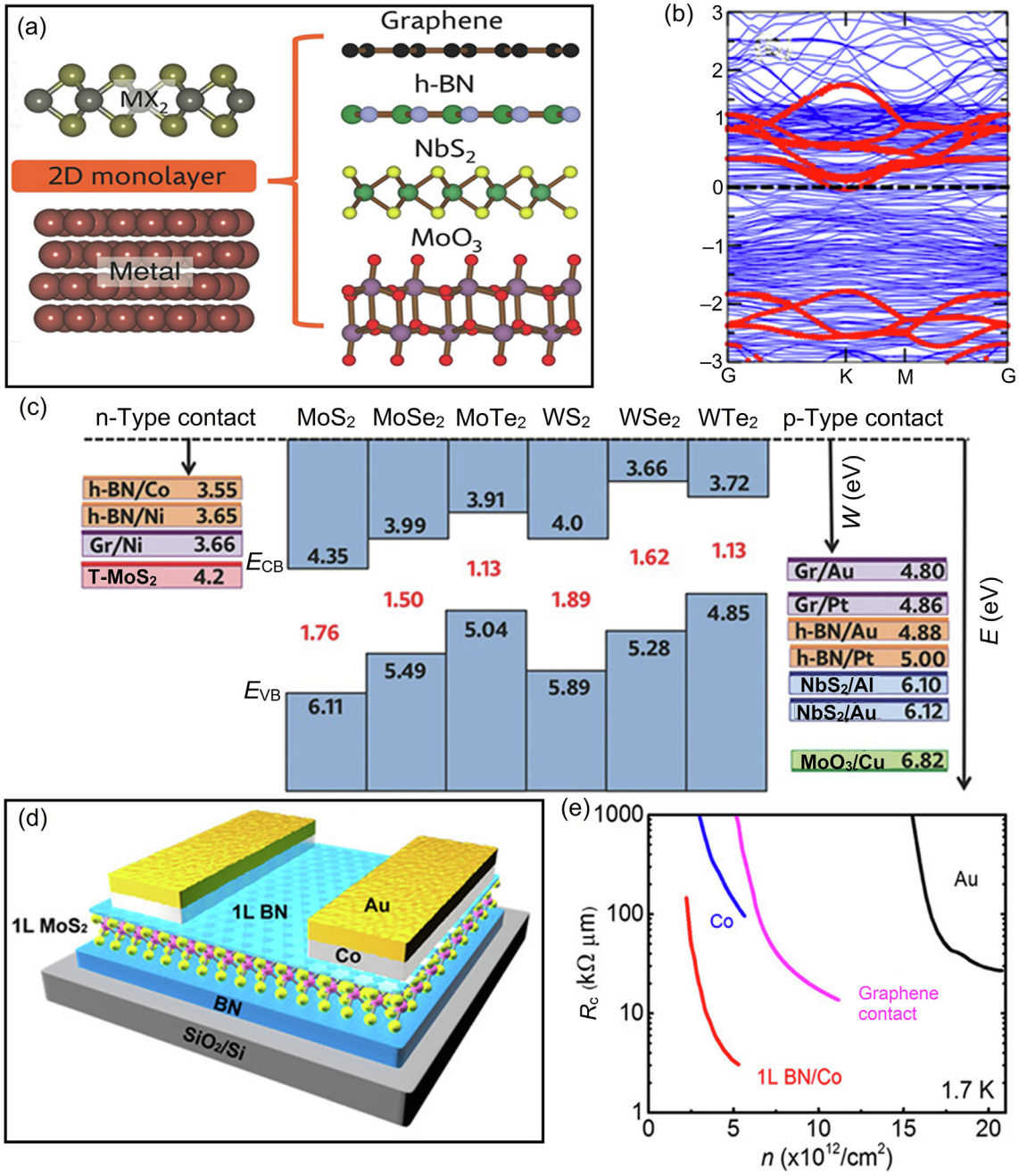

Fig. 3. (Color online) Inserting monolayer 2D materials at the MSJ interface to lift out the FLPE. (a) The schematic figure of using 2D monolayer materials as a buffer layer between the bulk metal and 2DS. Adapted from Ref. [41], Copyright © 2016 Wiley. (b) First-principle calculations suggest the weak interaction between Co contact and MoS_2 due to the existence of monolayer h-BN as buffer layer at the contact interface. Adapted from Ref. [40], Copyright © 2015 Wiley. (c) The band alignment to the TMD 2DS using the combination of different layered materialsand metal as contact [41]. (d) The schematic figure of device using the CoBN contact to achieve low-resistance contact. (e) The contact resistance of CoBN contact compared with other reported results, suggesting the best contact quality at low carrier density and at low temperature. Adapted from Ref. [42], Copyright © 2017 American Chemical Society.

given 2DS band. Second, ultrathin 2D contact such as graphene absorbs little light and can be used as a good transparent electrode in optoelectronic devices.

Using first-principle calculations, Liu et al. [46] showed the weak FLPE between 2D metallic materials and 2DS due to the suppression of metal-induced gap states (Fig. 4a). The calculated Schottky barrier for various metallic 2D materials as vdW contact to 2D H-MoS_2 is plotted with respect to the work function W (calibrated to Fermi level of H-MoS_2 in Fig. 4b). The result is in good agreement with Mott-Schottky rule, indicating the weak FLPE. The W of many more metallic 2D materials have been calculated and compared with the band alignment of 2DS, which gives a guideline to seek suitable vdW contact 2D materials for a given 2DS. Standing out from these metallic 2D materials, graphene is the most widely used vdW contact material because it is readily available, possesses an ultrahigh conductivity, and its work function W is around 4.4 eV (Fig. 4c), lying within the band gap of TMD 2DS, which facilitates efficient carrier injection and collection. Moreover, graphene has a low density of states, showing weak screening effect and its Fermi level or W is highly tunable by doping or gate voltage, which can be readily controlled to align to the band edges of 2DS to form a barrier-free vdW contact. This is

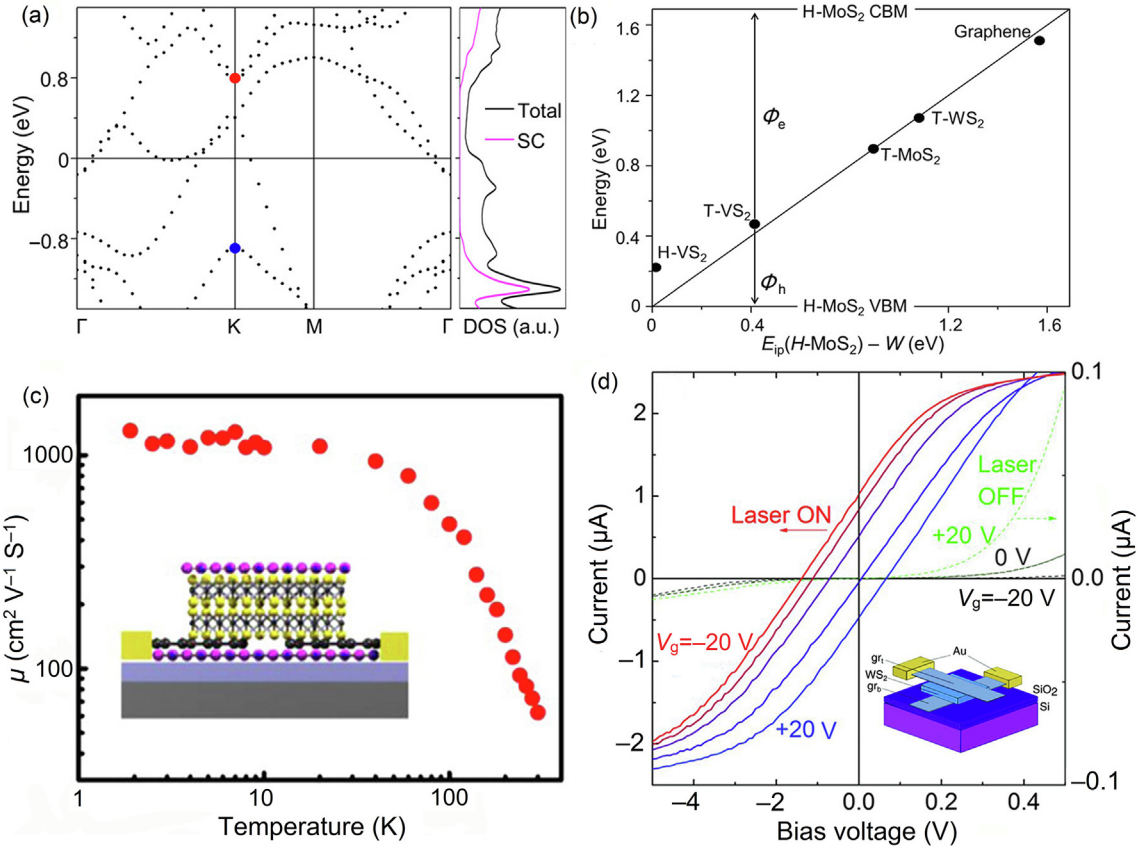

Fig. 4. (Color online) vdW contact using 2D metallic materials. (a) The band structure of monolayer H-MoS_2 with monolayer T-MoS_2 as vdW contact, showing that gap states primarily stem from the metallic T-MoS_2, implying the weak interactions at the interface. (b) The Schottky barrier using different metallic 2D materials to contact monolayer H-MoS_2, which is in good agreement to Schottky-Mott rule. Adapted from Ref. [46], Copyright © 2016 AAAS. (c) Graphene as vdW contact to MoS_2, with tunable Schottky barrier by the backgate. The resulting device shows high FET mobility due to the ohmic contact. Adapted from Ref. [47], Copyright © 2015 American Chemical Society. (d) The *I-V* curves of WS_2 device with graphene as top and bottom vdW contact in dark and under illumination with different back gate voltage, with the inset schematic figure of the device architecture. Adapted from Ref. [48], Copyright © 2013 AAAS.

demonstrated by Liu et al. [46] in an experimental work. Few-layer MoS_2 was stacked with two flakes of graphene and then sandwiched between h-BN for protection from contaminants. In such a way, the Fermi level of graphene flakes can be tuned by a back gate, see the inset schematic of Fig. 4c. A record-high field effect transistor mobility over 1,300 $cm^2\ V^{-1}\ s^{-1}$ is demonstrated in a two-terminal device at low temperature owing to the barrier-free contact and the protection structure. Graphene, as a good transparent electrode, has been widely used in the design of optoelectronic 2DS devices [24,48,49]. The device made of a monolayer of 2DS sandwiched between two graphene flakes as transparent vdW contact (Fig. 4d) showed strong light-matter interactions and its performance is tunable via the gate (Fig. 4d) or chemical doping. A built-in electric field can be induced via an asymmetric doping of the two graphene flakes or gate voltage to enable the photogenerated electron-hole separation [48].

The vdW contact can be readily developed thanks to the continuing discovery of metallic 2D materials, the advances of the vdW assemble techniques as well as the vdW epitaxial growth of 2DS and metallic 2D materials. The degenerately Nb-doped WSe_2 was also used as the vdW contact to WSe_2 for high performance devices [50,51]. The Fermi level of degenerately doped WSe_2 naturally aligns with the valence band of WSe_2 and leads to a contact of low Schottky energy barrier with WSe_2, which also proves to be effective in the reduction of contact resistance, even though the Fermi level of these metallic 2D materials is hardly tunable via gate voltage for its high carrier density. With the booming development of 2D materials, more 2D metallic materials have been synthesized and used as vdW contact to 2DS, either by vdW transferring or epitaxial growth. Using VS_2 flakes as vdW contact instead of Ni/Au, the contact resistance to monolayer MoS_2 reduced by 3/4 and leads to a significant increase of FET mobility [52]. Via epitaxial growth, the metallic 1 T' WTe_2 has been grown on WSe_2 monolayers, which is furthermore used as the FET contact, the Schottky barrier decreased from 126 to 71 meV in comparison to the Ti contact [53]. The devices with the vdW contact design opened possibilities to study many fundamental physical properties of 2D materials, and this is especially interesting in optoelectronic device design [49].

2.3. Edge contact

In the rest of this review, we focus on a totally different contact configuration: the edge contact. In the case of edge contact, the electrodes contact with 2DS only from the edges, which allows for the formation of covalent bonds between the 2DS and metallic contact [26] (Fig. 1). Generally speaking, the edge contact configuration can be classified into the bulk-2D edge contact and the 2D-2D edge contact.

2.3.1. Bulk-2D edge contact

The bulk-2D edge contact describes a contact configuration where the structure of the 2D materials is well defined so that the deposited metal atoms come to touch with the exposed edges

of 2D materials and form chemical bonds with the dangling atoms at the edges. The formation of bulk-2D edge contact requires a fine controlled process, but offers opportunities to fabricate the low-resistance contact to some specially designed devices. The good application scenario is that the 2D materials need to be encapsulated to enforce its stability or prevent the contaminants from environment and fabrication process, which are extremely important in the device design for fundamental studies.

In 2013, Wang et al. [54] demonstrated a graphene-based device with ultra-high electronic performance including ballistic transport of charge carriers over 15 μm at low temperature and its room-temperature mobility approaching the theoretical phonon-scattering limit. Though graphene is a semimetal, it is usually studied in a similar way as the 2DS since the behavior of its electric transport is extremely important while studying its intrinsic properties. In the device design, graphene was encapsulated between two h-BN flakes by a pick-up assembly technique, without introducing any observable contaminants [54]. To realize the electric transport measurement, the bulk-2D edge contact turned to be the only possible choice. As depicted in Fig. 5a, the stacked h-BN/graphene/h-BN heterostructure flake was etched to expose one or two atoms at the edges of graphene and then the metal was deposited to contact with the edges of graphene. The scanning transmission electron microscopy (STEM) image confirmed the true edge contact without evidence of metal diffusion into the vdW gaps and the electron energy loss spectroscopy (EELS) map shows good contact between graphene edge and Cr adhesion layer. The contact resistance was extracted from the plot of the device resistance with respect to the channel length, assuming that the whole device resistance is the sum of contact resistance and the channel resistance, i.e., $R = 2R_C(W) + rL/W$, where R_C is contact resistance, r is the graphene resistivity, and L and W are respectively the length and width of devices (2 μm), see the inset of Fig. 5c. The intercept of the plot indicates the contact resistance of the device as low as 150 Ω μm for n-type carriers and 80 Ω μm for p-type carriers at high density. Using ab initio calculations, it is found that the low contact resistance stems from shorter bonding distance between metal atoms and carbons of graphene, which leads to a larger orbital overlap than the conventional top contact configuration. Additionally, the graphene edges are exposed to oxygen in the etching process, possibly resulting in some interfacial species such as oxygen atoms between the Cr and carbons. These incorporation atoms at the edge contact can actually improve the bonding and decrease the contact resistance.

MoS_2 is an intensively studied 2DS due to its promising properties in fundamental studies and applications [2,3]. However, its intrinsic properties such as mobility have rarely been uncovered experimentally due to contaminants during the device fabrication process. In a device, where graphene was used as vdW contact to the encapsulated MoS_2 and the contact graphene was then connected with the external electrodes via the bulk-2D edge contact (Fig. 5d), Cui et al. [55] demonstrated the Hall mobility of 6-layer MoS_2 as high as 34,000 $cm^2 V^{-1} s^{-1}$ and the successful observation of Shubnikov-de Haas oscillations. This high mobility becomes experimentally observable due to the ultra-cleanness of the MoS_2 flakes and the design of low-resistance contact. The linear *I-V* plot of the device at different temperature indicates the good ohmic contact at both low temperature and room temperature. The

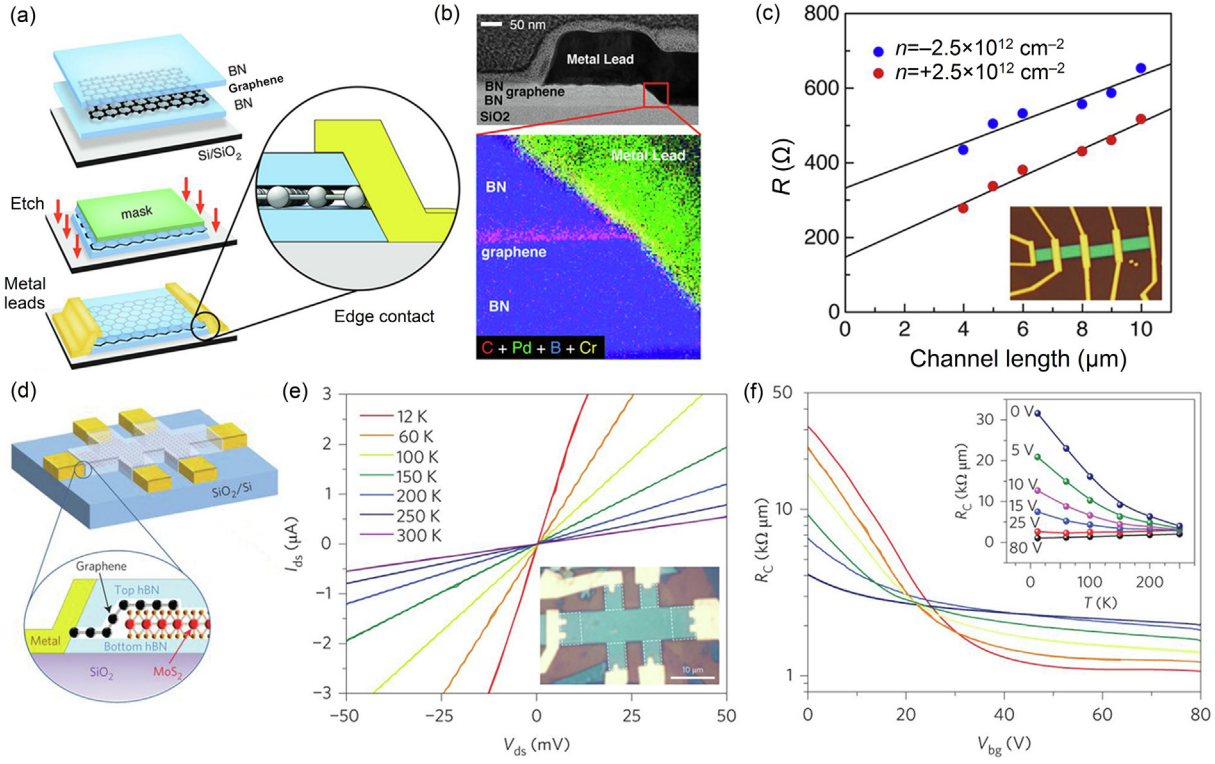

Fig. 5. (Color online) Bulk-2D edge contact. (a) The device fabrication process of bulk-2D edge contact to graphene encapsulated between two h-BN flakes. (b) The cross-section TEM image and EELS mapping of the edge contact. (c) The device resistance as a function of channel length, from which the contact resistance can be extracted. The inset figure is the optical image of device. Adapted from Ref. [54], Copyright © 2013 AAAS. (d) The device schematic figure of device where bulk-2D edge contact to graphene and vdW contact of graphene to MoS_2 are combined to achieve the low-resistance contact to encapsulated MoS_2. (e) Two terminal *I-V* measurement of the device at various temperatures with back gate of 80 V, in which the linear plots indicate a good ohmic contact at both room temperature and low temperature. (f) The contact resistance of a 4-layer MoS_2 device at different temperature from 250 to 12 K as a function of back gate voltage, in which the contact resistance is extracted by comparing the two-terminal measurement and the four-terminal measurement. Inset: contact resistance as a function of temperature at different back gate. Adapted from Ref. [55], Copyright © 2015 Springer Nature Publishing.

contact resistance can be extracted from the comparison of two-terminal and four-terminal measurement and its dependence on back gate voltage and temperature are plotted in Fig. 5f. The contact resistance is found to be tunable via the back gate, ranging between 2 and 20 kΩ μm at room temperature and between 0.7 and 10 kΩ μm under a high gate voltage. This contact resistance may mainly stem from the graphene vdW contact as the bulk-2D edge contact to graphene is merely one order of magnitude smaller. And the vdW contact resistance is sensitive to the back gate as we discussed previously.

In analogue to graphene, bulk-2D edge contact to the typical TMD semiconductor such as MoS_2 has also been exploited aiming to unlock the FLPE [56]. Using the similar processes for graphene, the metal was deposited to contact with the exposed edges of MoS_2 after the plasma etching. The polarity of MoS_2-based FET has been found to be tunable via the choice of contact metals with different work function W (n-type for Mo and Ti, p-type for Pd and Au). Hole mobility up to 330 and 432 $cm^2\ V^{-1}\ S^{-1}$ of Pd and Au edge-contacted FET has been demonstrated [56].

This strategy proves to be an appropriate, if not unique, solution to fabricating low-resistance electrical contact to the fully encapsulated 2D materials, which is crucially important to the fundamental studies and applications. For instance, the recent findings of Mott-insulator [57] and superconductivity [58] of magic-angle graphene also benefit from this low-resistance strategy of bulk-2D edge contact to study the intrinsic properties of twisted graphene encapsulated between two h-BN flakes. It can be expected that more devices dedicated to fundamental studies will employ this contact strategy.

2.3.2. 2D-2D edge contact

The realization of edge contact prerequisites the control of chemical bond formation in atomic scale at the edges of 2DS with one or two exposed atoms, which leads to the complicity in the fabrication process. Thanks to the burgeoning researches in 2D materials, some novel strategies lead to the rise of 2D-2D edge contact, where metallic 2D materials is electrically contacted with 2DS from the edges. These strategies, in contrast, can hardly been realized in Si-based semiconductor or III-V semiconductors because they rely on the specific properties of 2DS.

Unlike the conventional semiconductors, typical 2DS such as TMD materials (MoS_2, WSe_2, and $MoTe_2$) possess both the metallic and semiconducting phases. Additionally, only the chalcogenide atoms undergo a distortion movement in the phase transition, without breaking the chemical bonds, which results in a sharp phase boundary, free of defects and grain boundaries [59]. The 1 T-2H phase transition of TMD has been widely studied and a couple of treatment methods have been demonstrated to induce this phase transition for different TMD materials, including electrostatic doping [60], chemical treatment [61], plasma treatment [62], electron injection [63], laser irradiation [64], and applying strain [65]. Taking advantage of the phase transition in TMD, Kappera et al. [61] reported a method to controllably pattern the semiconducting 2H-MoS_2 and selectively transform the patterned area to metallic 1 T phase with chemical treatment, resulting in a 2D-2D edge contact of 1 T-2H junction (Fig. 6a). The 1 T-2H MoS_2 phase boundary is atomically sharp without observable defects. The metallic 1 T MoS_2 is used as electrodes and connected with external circuit, see the inset in Fig. 6b. The contact resistance is

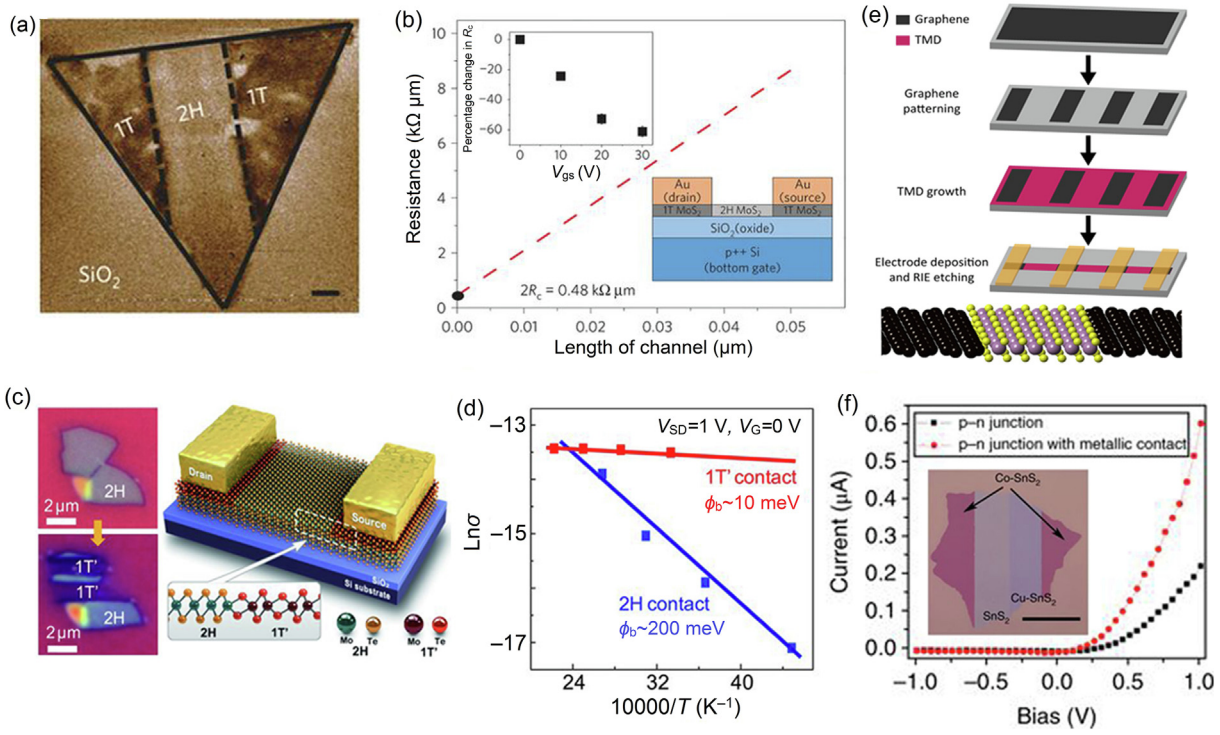

Fig. 6. (Color online) 2D-2D edge contact. (a) Electrostatic force microscopy phase image of a monolayer MoS_2 nanosheet showing the difference between locally patterned 2H (bright color) and 1 T (dark color) phases. (b) The low contact resistance extracted from the plot of device resistance versus channel length, which is indicated as the intercept, for the 2D-2D (1T-2H phase) edge contact. Inset, the schematic figures of the device. Adapted from Ref. [61], Copyright © 2014 Springer Nature Publishing. (c) The optical images of exfoliated 2H-$MoTe_2$ flake, before and after the treatment by laser irradiation, and the device structure using the 2D-2D edge contact. (d) The Arrhenius plots of the conductance, from which the Schottky barrier can be extracted. Adapted from Ref. [64], Copyright © 2015 AAAS. (e) Schematic figures of fabricating graphene-TMD edge contact via lateral epitaxial growth and the edge contact geometry. Adapted from Ref. [66], Copyright © 2016 American Chemical Society. (f) The comparison of rectification effect of PN junction (with as-grown bilayer SnS_2 and Cu-intercalated SnS_2 with conventional top contact (black dot) and 2D-2D edge contact made by locally Co intercalation. Inset, optical image of a single bilayer SnS_2 after spatially controlled intercalation, resulting in a PN junction with 2D-2D edge contact. Adapted from Ref. [67], Copyright © 2018 Springer Nature Publishing.

extracted using the aforementioned method and found to be 0.24 kΩ μm for the 2D-2D edge contact, with a decrease of a factor of 5 in comparison with the conventional top contact, as shown in Fig. 6b. The low-resistance contact to channel MoS_2 materials is obtained owing to the good match between the work function of 1 T phase and the conduction/valence band edge of 2H phase. It is worth noting that the contact resistance (0.24 kΩ μm) is orders of magnitude smaller than the resistance of shortest channel (~100 kΩ μm), which suggests some deficiency while extracting the real contact resistance. The idea of fabricating this 2D-2D edge conatct however sparked many other researh works. The locally patterned phase transition is also induced via argon plasma treatment, which is well tuned to lead the sliding of the top S atoms and avoid the etching effect to the material [62]. Similarly, a remarkable improvement of field effect transistor performance is demonstrated due to the application of the 2D-2D edge contact.

Relatively speaking, for $MoTe_2$, the phase transition to a metallic phase can be more readily induced than MoS_2 since its energy barrier of the phase transition is much smaller [68]. First-principles calculations showed that the ground-state energy difference between monolayer 2H and 1 T'-$MoTe_2$ is merely around 35 meV per formula unit, in contrast to over 500 meV for MoS_2 [66]. In this regard, it is reasonable to find more methods to provoke the phase transition of $MoTe_2$, among which, electrostatic gating [60], strain [65], electron injection [63], and laser irradiation [64] have been reported. Regarding the fabrication of 2D-2D edge contact, which requires the locally patterned control, the laser irradiation comes out to be more appropriate. Cho et al. [64] reported the fabrication of this 2D-2D edge contact to $MoTe_2$ via the controlled laser beam irradiation. As shown in Fig. 6c, the optical images demonstrate the exfoliated $MoTe_2$ flake, before and after the laser irradiation, and the schematic figure depicts the device structure, in which the 1 T'-$MoTe_2$ is used as the electrodes. The 2D-2D edge contact is stable up to 300 and the FET mobility of 50 times higher is demonstrated thanks to this contact optimization strategy. The Schottky barrier height Φ can be extracted via the temperature-dependent conductance measurement, which is found to be 10 meV for the 2D-2D edge contact and 200 meV for conventional top contact (Fig. 6d).

From a theoretical perspective, Liu et al. [69] investigated the electrical transport behaviors at the interface of H-MX_2 and T/T' MX_2 via the ab initio quantum transport simulations and found that the MIGS at this interface penetrate the SB and bridge the metallic phase and semiconducting phase, which provides a theoretical explanation for this high quality contact. In another work of ab initio calculations, Fan et al. [70] reported relations between the SB height at the contact interface for different semiconducting MX_2 and metallic MX_2 and also calculated the FET performance and exploited the possibilities of MX_2-based FET to meet the requirements of International Technology Roadmap for Semiconductors.

Apart from this method of fabricating metallic-semiconducting phase junction of TMD 2DS, the 2D-2D edge contact configuration can also be achieved by the heterogeneous lateral epitaxy growth of 2D metallic materials and 2DS. Guimarães et al. [66] reported the utilization of lateral graphene/TMD heterostructure via the epitaxial growth of monolayer TMD to edge contact the patterned monolayer graphene (Fig. 6e).

Wafer-scale monolayer graphene is etched and monolayer TMD is laterally grown from the edges of the patterned graphene via the highly controllable metal–organic chemical vapor deposition (MOCVD), which ensures the nucleation sites and growth behavior of TMD. Afterwards, the metal electrode is fabricated, which is followed by the final etching, resulting in an array of devices with graphene as edge contact. The edge contact resistance is measured to be 30 kΩ μm. The fabrication processes are compatible with the standard state-of-the-art fabrication of Si-based semiconductor techniques and this approach is scalable and applicable to other TMD materials, with MoS_2 and WS_2 particularly demonstrated as two examples. Afterwards, the lateral epitaxy of other metallic 2D and semiconducting 2D materials to form the edge contact are reported (1T'-$MoTe_2$ and H-$MoTe_2$ [71], VS_2 and MoS_2 [72], NbS_2 and WS_2 [73]).

Intercalation has proved to be a usual method to tune the properties of layered materials due to the vdW gaps of layered materials providing the intercalation channel. Via intercalating Co atoms into the vdW gap, Gong et al. [67] reported that the bilayer SnS_2 can be degenerately doped and turned to be metallic. As-grown bilayer SnS_2 is n-type semiconductor with S-vacancy, which can be locally transformed to be p-type semiconducting and metallic by spatially controlled intercalation of Cu and Co atoms, offering a promising method to fabricate a 2D-2D edge contact to n-type, p-type 2DS or PN junction. The rectification effect of the PN junction has been remarkably improved (larger on current), which is attributed to the 2D-2D edge contact with lower resistance compared with the conventional top contact of metal electrodes.

Generally, the key to achieving 2D-2D edge contact is to control the formation of chemical bonds at the 2D-2D MSJ to reduce the chemical disorder. New strategies to achieve the 2D-2D edge contact can be anticipated with our booming knowledge of 2D materials and the discovery of new 2DS in possession of new properties.

3. Summary and outlook

It is obvious that increasing research works are being devoted to dealing with the contact problem in 2DS devices, because it has become an obvious bottleneck towards better device performance and a roadblock for studying the intrinsic physical properties of 2D materials. The key to achieve barrier free contact is to engineer the MSJ interface thus eliminate the FLPE. Based on the three categories of contact configurations, we summarized the various strategies to construct the ohmic contact. These strategies significantly reduced the contact resistance but also showed some limitations in terms of device scaling up and process complexity.

In order to better illustrate the effects of different contact configurations as well as their limitations, we summarize the reported strategies concerning the improvement of electric contact to MoS_2, as showed in Table 1. Even though these strategies are demonstrated in the MoS2-based devices, all of them are in principle applicable to other 2DS.

In the top contact configuration, the FLPE can be lifted out via transferring the electrodes onto the top of 2DS instead of the conventional deposition-lifting process. The work function of the electrodes can be tuned via choosing different metals and the functionalities of 2DS devices can be controlled with the choice of different metals including the formation of low-resistance contact. This process however requires the transferring process, with limitations for the scale-up. Besides this method of transferring metal electrodes, it was found that the FLPE can be effectively relieved by inserting a buffer layer between the 2DS and bulk metal. Monolayer layered materials (graphene, h-BN) are firstly proposed theoretically and low-resistance contact were subsequently demonstrated in experiments. Regarding the h-BN as buffer layer, it not only optimizes the contact resistance but also acts as an encapsulating layer to the 2DS, making it possible to achieve a high mobility device. Nevertheless, the assembly of layered materials requires the vdW assembly process, which is hard to scale. Using molecules instead of layered materials turns to be a solution since the molecules spontaneously absorb onto the 2DS surface before the deposition of metal electrodes, which is a facile process and scalable. Nevertheless, the uniformity and reliability of the molecules turn to be a challenge. It is thus possible to improve

Table 1
Various reported strategies to improve the electric contact to monolayer or few-layer MoS_2, which can be classified into different contact configurations. The parameters not provided are indicated as *.

Contact configuration	Contact materials	Thickness of MoS_2	Transfer (Yes/No)	Contact resistance (kΩ μm)	Schottky barrier (meV)	Mobility (FET/Hall) (cm^2 V^{-1} s^{-1})	Refs.
Conventional top contact	Pt	10 nm	No	*	230	21	[36]
	Ni		No	*	150	90	
	Ti		No	*	50	125	
	Sc		No	*	30	184	
Using tunneling buffer layer	Co/h-BN	Monolayer	Yes	3 (gated)	16	1,250 @1.7 K	[42]
	Ni/h-BN	4–5 layers	Yes	1.8	31	321.4 @77 K	[43]
	Au/thiol-molecules	Greater than 20 nm	No	25.2	*	*	[44]
	Ni/graphene	16 nm	Yes	0.2	*	80	[45]
vdW contact	Graphene	1 and 20 layers	Yes	6–12	Free	1,300@1.9 K	[47]
Edge contact	1 T MoS_2	Monolayer	No	0.24	*	50	[61]
	Graphene	Monolayer	No	30	4 (gated)	*	[66]

the quality of molecule film on 2DS by self-assembly process or other more controllable techniques. It remains as an open question to develop a scalable process, allowing for the fabrication of ohmic contact using the buffer layer at the MSJ interface.

The vdW contact to the 2DS showed a few advantages in contrast to other contact configuration thanks to the atomic thinness of the contact in addition to the Fermi level depinning. First, graphene, as the widely used vdW contact electrode, the Fermi level of vdW electrodes can be tuned by the gate so that it is a priori adjustable to different 2DS for the band alignment. Second, the ultra-thin metallic vdW electrodes are almost transparent to the light of the whole spectrum, rendering it a good transparent electrodes in the design of optoelectronic devices. Third, the ultra-thin nature of vdW materials are of high flexibility, thus holds great potentials in the applications of flexible electronics. Assembling vdW contact materials with 2DS relies on the transfer process, which limits the possibility for the scale-up in device fabrication as well. Nevertheless, the development in the growth of vdW heterostructure and the advanced transfer techniques may open a new avenue for its scale-up. In any case, this contact strategy provides a great platform for the fundamental research in 2DS optoelectronic devices.

The successful development of edge contact to the encapsulated graphene remarkably extended our toolbox in designing ultra-clean devices, which is not only useful for the fundamental studies of graphene, twist-angle graphene, few-layer graphene, but also applicable to other 2DS as the graphene can be encapsulated with the 2DS and used as a tunable vdW contact to the 2DS. The development of this bulk-2D edge contact to the TMDs is still in its infancy. The electronic states at the edges with three atomic layers are probably more complicated in comparison with graphene. We can anticipate that more research works will be devoted to this research topic. For the TMD 2DS, the 2D-2D edge contact can be readily fabricated via the spatially controllable metallic-semiconducting phase transition and a couple of methods to tune the phase transition have been developed, capable of meeting the requirements in different application scenarios. Moreover, the formation of metallic-semiconducting phase homojunction holds the possibility for scaling up, which is actually limited by the size of the pristine materials.

Conflict of interest

The authors declare that they have no conflict of interest.

Acknowledgments

This work was supported by the National Natural Science Foundation of China (21825103, 51727809), the National Basic Research Program of China (2015CB932600), and the Fundamental Research Funds for the Central University (2019kfyXMBZ018). The authors are indebted for the kind permission from the corresponding publishers/authors to reproduce their materials, especially figures, used in this article.

Author contributions

K. Liu, H. Li and T. Zhai conceived the review topic. K. Liu and P. Luo arranged all the figures. K. Liu and T. Zhai wrote the manuscript in consultation with all the other authors. All authors modified the manuscript.

Appendix A. Supplementary data

Supplementary data to this article can be found online at https://doi.org/10.1016/j.scib.2019.06.021.

References

[1] Novoselov K, Mishchenko A, Carvalho A, et al. 2D materials and van der Waals heterostructures. Science 2016;353:aac9439.
[2] Mak KF, Lee C, Hone J, et al. Atomically thin MoS_2: a new direct-gap semiconductor. Phys Rev Lett 2010;105. 136805.
[3] Lopez-Sanchez O, Lembke D, Kayci M, et al. Ultrasensitive photodetectors based on monolayer MoS_2. Nat Nanotechnol 2013;8:497.
[4] Mak KF, Shan J. Photonics and optoelectronics of 2D semiconductor transition metal dichalcogenides. Nat Photon 2016;10:216.
[5] Zhu B, Zeng H, Dai J, et al. Anomalously robust valley polarization and valley coherence in bilayer WS_2. Proc Natl Acad Sci USA 2014;111:11606–11.
[6] Hafeez M, Gan L, Li H, et al. Chemical vapor deposition synthesis of ultrathin hexagonal $ReSe_2$ flakes for anisotropic Raman property and optoelectronic application. Adv Mater 2016;28:8296–301.
[7] Li L, Yu Y, Ye GJ, et al. Black phosphorus field-effect transistors. Nat Nanotechnol 2014;9:372.
[8] Wang X, Jones AM, Seyler KL, et al. Highly anisotropic and robust excitons in monolayer black phosphorus. Nat Nanotechnol 2015;10:517.
[9] Huang H, Jiang B, Zou X, et al. Black phosphorus electronics. Sci Bull 2019;64:1067–79.
[10] Li L, Wang W, Gong P, et al. 2D GeP: an unexploited low-symmetry semiconductor with strong in-plane anisotropy. Adv Mater 2018;30:1706771.
[11] Li L, Han W, Pi L, et al. Emerging in-plane anisotropic two-dimensional materials. InfoMat 2019;1:54–73.
[12] Tran V, Soklaski R, Liang Y, et al. Layer-controlled band gap and anisotropic excitons in few-layer black phosphorus. Phys Rev B 2014;89:235319.
[13] Wang G, Chernikov A, Glazov MM, et al. Colloquium: excitons in atomically thin transition metal dichalcogenides. Rev Mod Phys 2018;90:021001.
[14] Mak KF, Xiao D, Shan J. Light-valley interactions in 2D semiconductors. Nat Photon 2018;12:451.
[15] Luo P, Zhuge F, Zhang Q, et al. Doping engineering and functionalization of two-dimensional metal chalcogenides. Nanoscale Horiz 2019;4:26–51.
[16] Li D, Chen M, Sun Z, et al. Two-dimensional non-volatile programmable p-n junctions. Nat Nanotechnol 2017;12:901.
[17] Zhang F, Zhang H, Krylyuk S, et al. Electric-field induced structural transition in vertical $MoTe_2$-and $Mo_{1-x}W_xTe_2$-based resistive memories. Nat Mater 2019;18:55.

[18] Liu Y, Weiss NO, Duan X, et al. Van der Waals heterostructures and devices. Nat Rev Mater 2016;1:16042.
[19] Wang Y, Gan L, Chen J, et al. Achieving highly uniform two-dimensional PbI_2 flakes for photodetectors via space confined physical vapor deposition. Sci Bull 2017;62:1654–62.
[20] Wang S, Zhang DW, Zhou P. Two-dimensional materials for synaptic electronics and neuromorphic systems. Sci Bull 2019;64:1056–66.
[21] Cheng R, Yin L, Wang F, et al. Van der waals integration of 2D atomic crystals for advanced multifunctional devices. Sci Bull 2019;64:1033–5.
[22] Forsythe C, Zhou X, Watanabe K, et al. Band structure engineering of 2D materials using patterned dielectric superlattices. Nat Nanotechnol 2018;13:566.
[23] Yan J, Zhang Y, Kim P, et al. Electric field effect tuning of electron-phonon coupling in graphene. Phys Rev Lett 2007;98:166802.
[24] Lee CH, Lee GH, Van Der Zande AM, et al. Atomically thin p–n junctions with van der Waals heterointerfaces. Nat Nanotechnol 2014;9:676.
[25] Zhou S, Chen J, Gan L, et al. Scalable production of self-supported WS_2/CNFs by electrospinning as the anode for high-performance lithium-ion batteries. Sci Bull 2016;61:227–35.
[26] Allain A, Kang J, Banerjee K, et al. Electrical contacts to two-dimensional semiconductors. Nat Mater 2015;14:1195.
[27] Liu Y, Guo J, Zhu E, et al. Approaching the Schottky-Mott limit in van der Waals metal-semiconductor junctions. Nature 2018;577:696–700.
[28] Murthy AA, Stanev TK, Cain JD, et al. Intrinsic transport in 2D heterostructures mediated through h-BN tunneling contacts. Nano Lett 2018;18:2990–8.
[29] Kang J, Liu W, Sarkar D, et al. Computational study of metal contacts to monolayer transition-metal dichalcogenide Semiconductors. Phys Rev X 2014;4:031005.
[30] Bardeen J. Surface states and rectification at a metal semi-conductor contact. Phys Rev 1947;71:717.
[31] Tung RT. The physics and chemistry of the Schottky barrier height. Appl Phys Rev 2014;1:011304.
[32] Jiang B, Zou X, Su J, et al. Impact of thickness on contact issues for pinning effect in black phosphorus field effect transistors. Adv Funct Mater 2018;28:1801398.
[33] Schottky W. Zur halbleitertheorie der sperrschicht-und spitzengleichrichter. Z Phys A 1939;113:67–414.
[34] Mott N. The theory of crystal rectifiers. Proc R Soc Lond A 1939;171:27–38.
[35] Kim C, Moon I, Lee D, et al. fermi level pinning at electrical metal contacts of monolayer molybdenum dichalcogenides. ACS Nano 2017;11:1588–96.
[36] Kim GS, Kim SH, Park J, et al. Schottky barrier height engineering for electrical contacts of multilayered MoS_2 Transistors with reduction of metal-induced gap states. ACS Nano 2018;12:6292–300.
[37] Chen JR, Odenthal PM, Swartz AG, et al. Control of Schottky barriers insingle layer MoS_2 transistors with ferromagnetic contacts. Nano Lett 2013;13:3106–10.
[38] Lee S, Tang A, Aloni S, et al. statistical study on the schottky barrier reduction of tunneling contacts to CVD synthesized MoS_2. Nano Lett 2015;16:276–81.
[39] Dankert A, Langouche L, Kamalakar MV, et al. High-performance molybdenum disulfide field-effect transistors with spin tunnel contacts. ACS Nano 2014;8:476–82.
[40] Farmanbar M, Brocks G. Controlling the Schottky barrier at MoS_2 metal contacts by inserting a BN monolayer. Phys Rev B 2015;91:161304.
[41] Farmanbar M, Brocks G. Ohmic contacts to 2D semiconductors through van der Waals bonding. Adv Electon Mater 2016;2:1500405.
[42] Cui X, Shih EM, Jauregui LA, et al. Low-temperature ohmic contact to monolayer MoS_2 by van der Waals bonded Co/h-BN electrodes. Nano Lett 2017;17:4781–6.
[43] Wang J, Yao Q, Huang CW, et al. High mobility MoS_2 transistor with low schottky barrier contact by using atomic thick h–BN as a tunneling layer. Adv Mater 2016;28:8302–8.
[44] Leong WS, Luo X, Li Y, et al. low resistance metal contacts to mos_2 devices with nickel-etched-graphene electrodes. ACS Nano 2014;9:869–77.
[45] Cho K, Pak J, Kim JK, et al. contact-engineered electrical properties of mos_2 field effect transistors via selectively deposited thiol-molecules. Adv Mater 2018;30:1705540.
[46] Liu Y, Stradins P, Wei SH. Van der Waals metal-semiconductor junction: weak Fermi level pinning enables effective tuning of Schottky barrier. Sci Adv 2016;2. e1600069.
[47] Liu Y, Wu H, Cheng HC, et al. Toward barrier free contact to molybdenum disulfide using graphene electrodes. Nano Lett 2015;15:3030–4.
[48] Britnell L, Ribeiro R, Eckmann A, et al. Strong light-matter interactions in heterostructures of atomically thin films. Science 2013;340:1311–4.
[49] Massicotte M, Schmidt P, Vialla F, et al. Picosecond photoresponse in van der Waals heterostructures. Nat Nanotechnol 2016;11:42.
[50] Chuang HJ, Chamlagain B, Koehler M, et al. low-resistance 2D/2D ohmic contacts: a universal approach to high-performance WSe_2, MoS_2, and $MoSe_2$ transistors. Nano Lett 2016;16:1896–902.
[51] Wang T, Andrews K, Bowman A, et al. High-performance WSe_2 phototransistors with 2D/2D ohmic contacts. Nano Lett 2018;18:2766–71.
[52] Ji Q, Li C, Wang J, et al. Metallic vanadium disulfide nanosheets as a platform material for multifunctional electrode applications. Nano Lett 2017;17:4908–16.
[53] Lee CS, Oh SJ, Seo SY, et al. Epitaxial van der Waals contacts between transition-metal dichalcogenide monolayer polymorphs. Nano Lett 2019;19:1814–20.
[54] Wang L, Meric I, Huang P, et al. One-dimensional electrical contact to a two-dimensional material. Science 2013;342:614–7.
[55] Cui X, Lee GH, Kim YD, et al. Multi-terminal transport measurements of MoS_2 using a van der Waals heterostructure device platform. Nat Nanotechnol 2015;10:534.
[56] Yang Z, Kim C, Lee KY, et al. A Fermi-level-pinning-free 1D electrical contact at the intrinsic 2D MoS_2-metal junction. Adv Mater 2019;31:1808231.
[57] Cao Y, Fatemi V, Demir A, et al. Correlated insulator behaviour at half-filling in magic-angle graphene superlattices. Nature 2018;556:80.
[58] Cao Y, Fatemi V, Fang S, et al. Unconventional superconductivity in magic-angle graphene superlattices. Nature 2018;556:43.
[59] Yang H, Kim SW, Chhowalla M, et al. Structural and quantum-state phase transitions in van der Waals layered materials. Nat Phys 2017;13:931.
[60] Wang Y, Xiao J, Zhu H, et al. Structural phase transition in monolayer $MoTe_2$ driven by electrostatic doping. Nature 2017;550:487.
[61] Kappera R, Voiry D, Yalcin SE, et al. Phase-engineered low-resistance contacts for ultrathin MoS_2 transistors. Nat Mater 2014;13:1128.
[62] Zhu J, Wang Z, Yu H, et al. Argon Plasma induced phase transition in monolayer MoS_2. J Am Chem Soc 2017;139:10216–9.
[63] Kim S, Song S, Park J, et al. Long-range lattice engineering of $MoTe_2$ by a 2D electride. Nano Lett 2017;17:3363–8.
[64] Cho S, Kim S, Kim JH, et al. Phase patterning for ohmic homojunction contact in $MoTe_2$. Science 2015;349:625–8.
[65] Song S, Keum DH, Cho S, et al. room temperature semiconductor-metal transition of $MoTe_2$ thin films engineered by strain. Nano Lett 2015;16:188–93.
[66] Guimaraes MH, Gao H, Han Y, et al. Atomically thin ohmic edge contacts between two-dimensional materials. ACS Nano 2016;10:6392–9.
[67] Gong Y, Yuan H, Wu CL, et al. Spatially controlled doping of two-dimensional SnS_2 through intercalation for electronics. Nat Nanotechnol 2018;13:294.
[68] Duerloo KAN, Li Y, Reed EJ. Structural phase transitions in two-dimensional Mo- and W-dichalcogenide monolayers. Nat Commun 2014;5:4214.
[69] Liu S, Li J, Shi B, et al. Gate-tunable interfacial properties of in-plane ML MX_2 1T′-2H heterojunctions. J Mater Chem C 2018;6:5651–61.
[70] Fan ZQ, Jiang XW, Chen J, et al. Improving performances of in-plane transition-metal dichalcogenide Schottky barrier field-effect Transistors. ACS Appl Mater Interfaces 2018;10:19271–7.
[71] Sung JH, Heo H, Si S, et al. Coplanar semiconductor–metal circuitry defined on few-layer $MoTe_2$ via polymorphic heteroepitaxy. Nat Nanotechnol 2017;12:1064.
[72] Leong WS, Ji Q, Mao N, et al. synthetic lateral metal-semiconductor heterostructures of transition metal disulfides. J Am Chem Soc 2018;140:12354–8.
[73] Zhang Y, Yin L, Chu J, et al. edge-epitaxial growth of 2d NbS_2-WS_2 lateral metal-semiconductor heterostructures. Adv Mater 2018;30:1803665.

Kailang Liu received his B.S. degree from Huazhong University of Science and Technology (HUST) in 2010, his Master's degree from the Institute of Metal Research, Chinese Academy of Sciences in 2013 and his Ph.D. degree in solid-state matter and physics from Ecole Centrale Marseille in France in 2017. He is currently a postdoc researcher in Prof. Tianyou Zhai's group in HUST and focuses his research interests on the 2D materials and devices.

Tianyou Zhai received his B.S. degree in Chemistry from Zhengzhou University in 2003, and his Ph.D. degree in Physical Chemistry from the Institute of Chemistry, Chinese Academy of Sciences (ICCAS) under the supervision of Prof. Jiannian Yao in 2008. Afterwards he joined in National Institute for Materials Science (NIMS) as a JSPS postdoctoral fellow of Prof. Yoshio Bando's group and then as an ICYS-MANA researcher within NIMS. Currently, he is a Chief Professor of School of Materials Science and Engineering, Huazhong University of Science and Technology (HUST). His research interests include the controlled synthesis and exploration of fundamental physical properties of inorganic functional nanomaterials, as well as their promising applications in energy science, electronics and optoelectronics.